



Third Edition  
**MECHANICS OF MATERIALS**

**FERDINAND P. BEER**

Lehigh University

**E. RUSSELL JOHNSTON, JR.**

University of Connecticut

**JOHN T. DEWOLF**

University of Connecticut

**BEST AVAILABLE COPY**



Boston Burr Ridge, IL Dubuque, IA Madison, WI New York San Francisco St. Louis  
Bangkok Bogotá Caracas Kuala Lumpur Lisbon London Madrid Mexico City  
Milan Montreal New Delhi Santiago Seoul Singapore Sydney Taipei Toronto

# McGraw-Hill Higher Education

A Division of The McGraw-Hill Companies

*The photograph on the cover shows a steel wide-flange column being tested in the five-million-pound universal testing machine at Lehigh University, Bethlehem, Pennsylvania. (Courtesy of Fritz Engineering Laboratory.)*

## MECHANICS OF MATERIALS

Published by McGraw-Hill, an imprint of The McGraw-Hill Companies, Inc. 1221 Avenue of the Americas, New York, NY, 10020. Copyright © 2001, 1992, 1981, by The McGraw-Hill Companies, Inc. All rights reserved. No part of this publication may be reproduced or distributed in any form or by any means, or stored in a database or retrieval system, without the prior written consent of The McGraw-Hill Companies, Inc., including, but not limited to, in any network or other electronic storage or transmission, or broadcast for distance learning.

Some ancillaries, including electronic and print components, may not be available to customers outside the United States.

This book is printed on acid-free paper.

International 2 3 4 5 6 7 8 9 0 VNH/VNH 0 9 8 7 6 5 4 3 2 1  
Domestic 2 3 4 5 6 7 8 9 0 VNH/VNH 0 9 8 7 6 5 4 3 2 1

ISBN 0-07-365935-5

Publisher: Elizabeth A. Jones  
Senior sponsoring editor: Jonathan Plant  
Associate editor: Debra Matteson  
Marketing manager: Ann Caven  
Project manager: Kimberly D. Hooker  
Lead production supervisor: Heather Burbridge  
Director, design BR: Keith McPherson  
Manager, publication services: Ira Roberts  
Photo researcher: Sabina Dowell  
Senior supplement coordinator: Carol Loreth  
Senior producer/developer, media technology: Phillip Meek  
Cover design: Michael Warrell  
Cover photo: Courtesy of Fritz Engineering Laboratory  
Interior design: Maureen McCutcheon/TECHBOOKS  
Compositor: TECHBOOKS/Production Manager: E. Gail Downey  
Typeface: 10/12 New Caledonia  
Printer: Von Hoffmann Press, Inc.

## Library of Congress Cataloging-in-Publication Data

Beer, Ferdinand Pierre, 1915–  
Mechanics of materials / Ferdinand P. Beer, E. Russell Johnston, Jr., John T. DeWolf.—  
3rd ed.  
p. cm.  
ISBN 0-07-365935-5  
I. Strength of materials. I. Johnston, E. Russell (Elwood Russell), 1925– II. DeWolf, John T., 1943– III. Title.  
TA405 .B39 2002  
620.1'12—dc21

2001030518

INTERNATIONAL EDITION ISBN 0-07-112167-6

Copyright © 2002 Exclusive rights by The McGraw-Hill Companies, Inc., for manufacture and export. This book cannot be re-exported from the country to which it is sold by McGraw-Hill. The International Edition is not available in North America.

www.mhhe.com

nent of the shearing stress exerted on a face perpendicular to the  $y$  axis. From the remaining two equations (1.20), we derive in a similar manner the relations

$$\tau_{yz} = \tau_{zy} \quad \tau_{zx} = \tau_{xz} \quad (1.22)$$

We conclude from Eqs. (1.21) and (1.22) that only six stress components are required to define the condition of stress at a given point  $Q$ , instead of nine as originally assumed. These six components are  $\sigma_x, \sigma_y, \sigma_z, \tau_{xy}, \tau_{yz},$  and  $\tau_{zx}$ . We also note that, at a given point, *shear cannot take place in one plane only*; an equal shearing stress must be exerted on another plane perpendicular to the first one. For example, considering again the bolt of Fig. 1.29 and a small cube at the center  $Q$  of the bolt (Fig. 1.39a), we find that shearing stresses of equal magnitude must be exerted on the two horizontal faces of the cube and on the two faces which are perpendicular to the forces  $P$  and  $P'$  (Fig. 1.39b).

Before concluding our discussion of stress components, let us consider again the case of a member under axial loading. If we consider a small cube with faces respectively parallel to the faces of the member and recall the results obtained in Sec. 1.11, we find that the conditions of stress in the member may be described as shown in Fig. 1.40a; the only stresses are normal stresses  $\sigma_x$  exerted on the faces of the cube which are perpendicular to the  $x$  axis. However, if the small cube is rotated by  $45^\circ$  about the  $z$  axis so that its new orientation matches the orientation of the sections considered in Fig. 1.31c and d, we conclude that normal and shearing stresses of equal magnitude are exerted on four faces of the cube (Fig. 1.40b). We thus observe that the same loading condition may lead to different interpretations of the stress situation at a given point, depending upon the orientation of the element considered. More will be said about this in Chap 7.

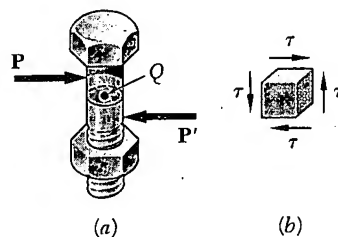


Fig. 1.39

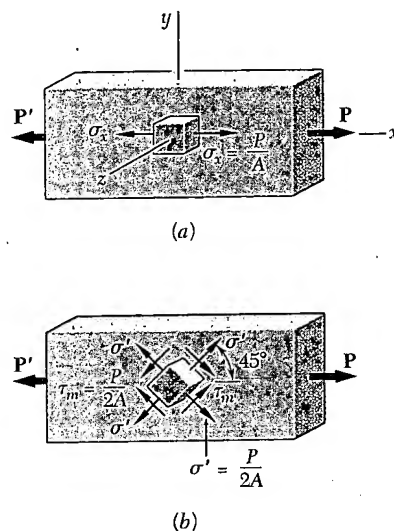


Fig. 1.40

### 1.13. DESIGN CONSIDERATIONS

In the preceding sections you learned to determine the stresses in rods, bolts, and pins under simple loading conditions. In later chapters you will learn to determine stresses in more complex situations. In engineering applications, however, the determination of stresses is seldom an end in itself. Rather, the knowledge of stresses is used by engineers to assist in their most important task, namely, the design of structures and machines that will safely and economically perform a specified function.

**a. Determination of the Ultimate Strength of a Material.** An important element to be considered by a designer is how the material that has been selected will behave under a load. For a given material this is determined by performing specific tests on prepared samples of the material. For example, a test specimen of steel may be prepared and placed in a laboratory testing machine to be subjected to a known centric axial tensile force, as described in Sec. 2.3. As the magnitude of the force is increased, various changes in the specimen are measured, for example, changes in its length and its diameter. Eventually the largest

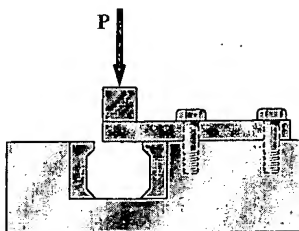


Fig. 1.41

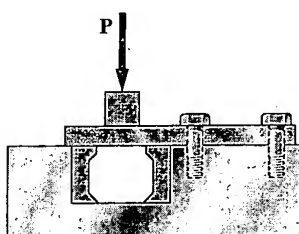


Fig. 1.42

force which may be applied to the specimen is reached, and the specimen either breaks or begins to carry less load. This largest force is called the *ultimate load* for the test specimen and is denoted by  $P_U$ . Since the applied load is centric, we may divide the ultimate load by the original cross-sectional area of the rod to obtain the *ultimate normal stress* of the material used. This stress, also known as the *ultimate strength in tension* of the material, is

$$\sigma_U = \frac{P_U}{A} \quad (1.23)$$

Several test procedures are available to determine the *ultimate shearing stress*, or *ultimate strength in shear*, of a material. The one most commonly used involves the twisting of a circular tube (Sec. 3.5). A more direct, if less accurate, procedure consists in clamping a rectangular or round bar in a shear tool (Fig. 1.41) and applying an increasing load  $P$  until the ultimate load  $P_U$  for single shear is obtained. If the free end of the specimen rests on both of the hardened dies (Fig. 1.42), the ultimate load for double shear is obtained. In either case, the ultimate shearing stress  $\tau_U$  is obtained by dividing the ultimate load by the total area over which shear has taken place. We recall that, in the case of single shear, this area is the cross-sectional area  $A$  of the specimen, while in double shear it is equal to twice the cross-sectional area.

**b. Allowable Load and Allowable Stress; Factor of Safety.** The maximum load that a structural member or a machine component will be allowed to carry under normal conditions of utilization is considerably smaller than the ultimate load. This smaller load is referred to as the *allowable load* and, sometimes; as the *working load* or *design load*. Thus, only a fraction of the ultimate-load capacity of the member is utilized when the allowable load is applied. The remaining portion of the load-carrying capacity of the member is kept in reserve to assure its safe performance. The ratio of the ultimate load to the allowable load is used to define the *factor of safety*.† We have

$$\text{Factor of safety} = F.S. = \frac{\text{ultimate load}}{\text{allowable load}} \quad (1.24)$$

An alternative definition of the factor of safety is based on the use of stresses:

$$\text{Factor of safety} = F.S. = \frac{\text{ultimate stress}}{\text{allowable stress}} \quad (1.25)$$

The two expressions given for the factor of safety in Eqs. (1.24) and (1.25) are identical when a linear relationship exists between the load and the stress. In most engineering applications, however, this relationship ceases to be linear as the load approaches its ultimate value, and the factor of safety obtained from Eq. (1.25) does not provide a

†In some fields of engineering, notably aeronautical engineering, the *margin of safety* is used in place of the factor of safety. The margin of safety is defined as the factor of safety minus one; that is, margin of safety =  $F.S. - 1.00$ .

Since deformation and length are expressed in the same units, the normal strain  $\epsilon$  obtained by dividing  $\delta$  by  $L$  (or  $d\delta$  by  $dx$ ) is a *dimensionless quantity*. Thus, the same numerical value is obtained for the normal strain in a given member, whether SI metric units or U.S. customary units are used. Consider, for instance, a bar of length  $L = 0.600$  m and uniform cross section, which undergoes a deformation  $\delta = 150 \times 10^{-6}$  m. The corresponding strain is

$$\epsilon = \frac{\delta}{L} = \frac{150 \times 10^{-6} \text{ m}}{0.600 \text{ m}} = 250 \times 10^{-6} \text{ m/m} = 250 \times 10^{-6}$$

Note that the deformation could have been expressed in micrometers:  $\delta = 150 \mu\text{m}$ . We would then have written

$$\epsilon = \frac{\delta}{L} = \frac{150 \mu\text{m}}{0.600 \text{ m}} = 250 \mu\text{m/m} = 250 \mu$$

and read the answer as “250 micros.” If U.S. customary units are used, the length and deformation of the same bar are, respectively,  $L = 23.6$  in. and  $\delta = 5.91 \times 10^{-3}$  in. The corresponding strain is

$$\epsilon = \frac{\delta}{L} = \frac{5.91 \times 10^{-3} \text{ in.}}{23.6 \text{ in.}} = 250 \times 10^{-6} \text{ in./in.}$$

which is the same value that we found using SI units. It is customary, however, when lengths and deformations are expressed in inches or microinches ( $\mu\text{in.}$ ), to keep the original units in the expression obtained for the strain. Thus, in our example, the strain would be recorded as  $\epsilon = 250 \times 10^{-6} \text{ in./in.}$  or, alternatively, as  $\epsilon = 250 \mu\text{in./in.}$

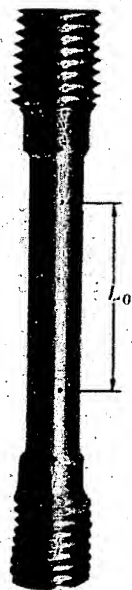


Fig. 2.6 Typical tensile-test specimen.

### 2.3. STRESS-STRAIN DIAGRAM

We saw in Sec. 2.2 that the diagram representing the relation between stress and strain in a given material is an important characteristic of the material. To obtain the stress-strain diagram of a material, one usually conducts a *tensile test* on a specimen of the material. One type of specimen commonly used is shown in Fig. 2.6. The cross-sectional area of the cylindrical central portion of the specimen has been accurately determined and two gage marks have been inscribed on that portion at a distance  $L_0$  from each other. The distance  $L_0$  is known as the *gage length* of the specimen.

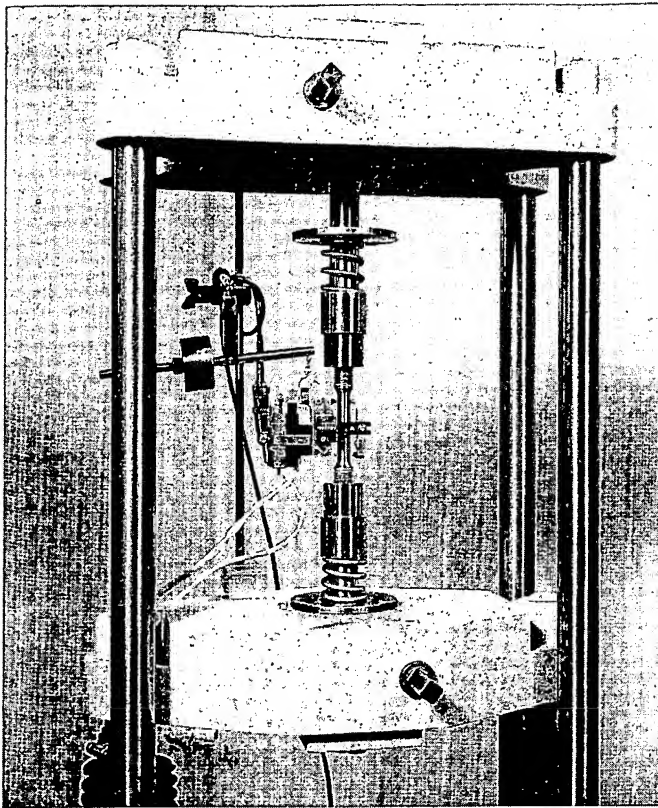


Fig. 2.7 This machine is used to test tensile test specimens, such as those shown in this chapter.

The test specimen is then placed in a testing machine (Fig. 2.7), which is used to apply a centric load  $P$ . As the load  $P$  increases, the distance  $L$  between the two gage marks also increases (Fig. 2.8). The distance  $L$  is measured with a dial gage, and the elongation  $\delta = L - L_0$  is recorded for each value of  $P$ . A second dial gage is often used simultaneously to measure and record the change in diameter of the specimen. From each pair of readings  $P$  and  $\delta$ , the stress  $\sigma$  is computed by dividing  $P$  by the original cross-sectional area  $A_0$  of the specimen, and the strain  $\epsilon$  by dividing the elongation  $\delta$  by the original distance  $L_0$  between the two gage marks. The stress-strain diagram may then be obtained by plotting  $\epsilon$  as an abscissa and  $\sigma$  as an ordinate.

Stress-strain diagrams of various materials vary widely, and different tensile tests conducted on the same material may yield different results, depending upon the temperature of the specimen and the speed of loading. It is possible, however, to distinguish some common characteristics among the stress-strain diagrams of various groups of materials and to divide materials into two broad categories on the basis of these characteristics, namely, the *ductile* materials and the *brittle* materials.

Ductile materials, which comprise structural steel, as well as many alloys of other metals, are characterized by their ability to *yield* at normal temperatures. As the specimen is subjected to an increasing load, its length first increases linearly with the load and at a very slow rate. Thus, the initial portion of the stress-strain diagram is a straight line



Fig. 2.8 Test specimen with tensile load.

Fig. 2.9 Stress-strain diagrams of two typical ductile materials.

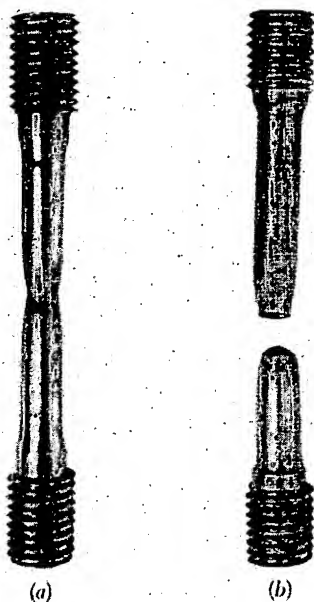
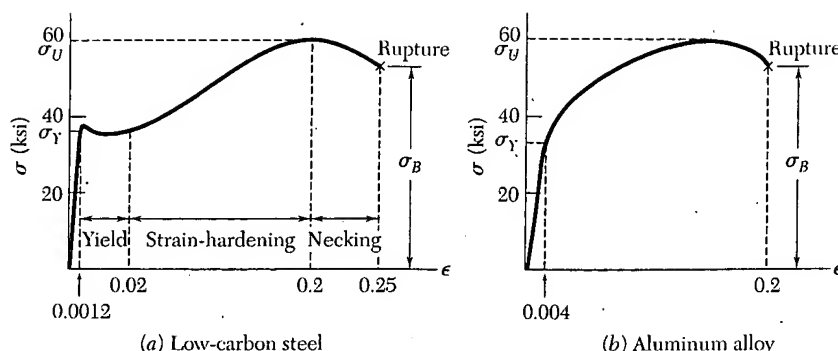


Fig. 2.10 Tested specimen of a ductile material.

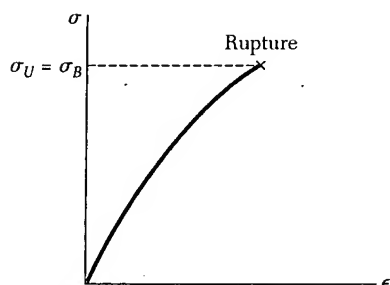


Fig. 2.11 Stress-strain diagram for a typical brittle material.

with a steep slope (Fig. 2.9). However, after a critical value  $\sigma_Y$  of the stress has been reached, the specimen undergoes a large deformation with a relatively small increase in the applied load. This deformation is caused by slippage of the material along oblique surfaces and is due, therefore, primarily to shearing stresses. As we can note from the stress-strain diagrams of two typical ductile materials (Fig. 2.9), the elongation of the specimen after it has started to yield can be 200 times as large as its deformation before yield. After a certain maximum value of the load has been reached, the diameter of a portion of the specimen begins to decrease, because of local instability (Fig. 2.10a). This phenomenon is known as *necking*. After necking has begun, somewhat lower loads are sufficient to keep the specimen elongating further, until it finally ruptures (Fig. 2.10b). We note that rupture occurs along a cone-shaped surface which forms an angle of approximately  $45^\circ$  with the original surface of the specimen. This indicates that shear is primarily responsible for the failure of ductile materials, and confirms the fact that, under an axial load, shearing stresses are largest on surfaces forming an angle of  $45^\circ$  with the load (cf. Sec. 1.11). The stress  $\sigma_Y$  at which yield is initiated is called the *yield strength* of the material, the stress  $\sigma_U$  corresponding to the maximum load applied to the specimen is known as the *ultimate strength*, and the stress  $\sigma_B$  corresponding to rupture is called the *breaking strength*.

Brittle materials, which comprise cast iron, glass, and stone, are characterized by the fact that rupture occurs without any noticeable prior change in the rate of elongation (Fig. 2.11). Thus, for brittle materials, there is no difference between the ultimate strength and the breaking strength. Also, the strain at the time of rupture is much smaller for brittle than for ductile materials. From Fig. 2.12, we note the absence of any necking of the specimen in the case of a brittle material, and observe that rupture occurs along a surface perpendicular to the load. We conclude from this observation that normal stresses are primarily responsible for the failure of brittle materials.†

†The tensile tests described in this section were assumed to be conducted at normal temperatures. However, a material that is ductile at normal temperatures may display the characteristics of a brittle material at very low temperatures, while a normally brittle material may behave in a ductile fashion at very high temperatures. At temperatures other than normal, therefore, one should refer to a *material in a ductile state* or to a *material in a brittle state*, rather than to a ductile or brittle material.



Fig. 2.12 Tested specimen of a brittle material.

The stress-strain diagrams of Fig. 2.9 show that structural steel and aluminum, while both ductile, have different yield characteristics. In the case of structural steel (Fig. 2.9a), the stress remains constant over a large range of values of the strain after the onset of yield. Later the stress must be increased to keep elongating the specimen, until the maximum value  $\sigma_U$  has been reached. This is due to a property of the material known as strain-hardening. The yield strength of structural steel can be determined during the tensile test by watching the load shown on the display of the testing machine. After increasing steadily, the load is observed to suddenly drop to a slightly lower value, which is maintained for a certain period while the specimen keeps elongating. In a very carefully conducted test, one may be able to distinguish between the *upper yield point*, which corresponds to the load reached just before yield starts, and the *lower yield point*, which corresponds to the load required to maintain yield. Since the upper yield point is transient, the lower yield point should be used to determine the yield strength of the material.

In the case of aluminum (Fig. 2.9b) and of many other ductile materials, the onset of yield is not characterized by a horizontal portion of the stress-strain curve. Instead, the stress keeps increasing—although not linearly—until the ultimate strength is reached. Necking then begins, leading eventually to rupture. For such materials, the yield strength  $\sigma_Y$  can be defined by the offset method. The yield strength at 0.2% offset, for example, is obtained by drawing through the point of the horizontal axis of abscissa  $\epsilon = 0.2\%$  (or  $\epsilon = 0.002$ ), a line parallel to the initial straight-line portion of the stress-strain diagram (Fig. 2.13). The stress  $\sigma_Y$  corresponding to the point Y obtained in this fashion is defined as the yield strength at 0.2% offset.

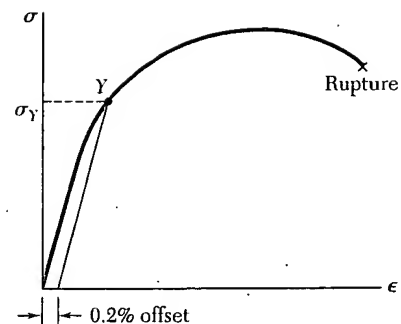


Fig. 2.13 Determination of yield strength by offset method.



A standard measure of the ductility of a material is its *percent elongation*, which is defined as

$$\text{Percent elongation} = 100 \frac{L_B - L_0}{L_0}$$

where  $L_0$  and  $L_B$  denote, respectively, the initial length of the tensile test specimen and its final length at rupture. The specified minimum elongation for a 2-in. gage length for commonly used steels with yield strengths up to 50 ksi is 21%. We note that this means that the average strain at rupture should be at least 0.21 in./in.

Another measure of ductility which is sometimes used is the *percent reduction in area*, defined as

$$\text{Percent reduction in area} = 100 \frac{A_0 - A_B}{A_0}$$

where  $A_0$  and  $A_B$  denote, respectively, the initial cross-sectional area of the specimen and its minimum cross-sectional area at rupture. For structural steel, percent reductions in area of 60 to 70 percent are common.

Thus far, we have discussed only tensile tests. If a specimen made of a ductile material were loaded in compression instead of tension, the stress-strain curve obtained would be essentially the same through its initial straight-line portion and through the beginning of the portion corresponding to yield and strain-hardening. Particularly noteworthy is the fact that for a given steel, the yield strength is the same in both tension and compression. For larger values of the strain, the tension and compression stress-strain curves diverge, and it should be noted that necking cannot occur in compression. For most brittle materials, one finds that the ultimate strength in compression is much larger than the ultimate strength in tension. This is due to the presence of flaws, such as microscopic cracks or cavities, which tend to weaken the material in tension, while not appreciably affecting its resistance to compressive failure.

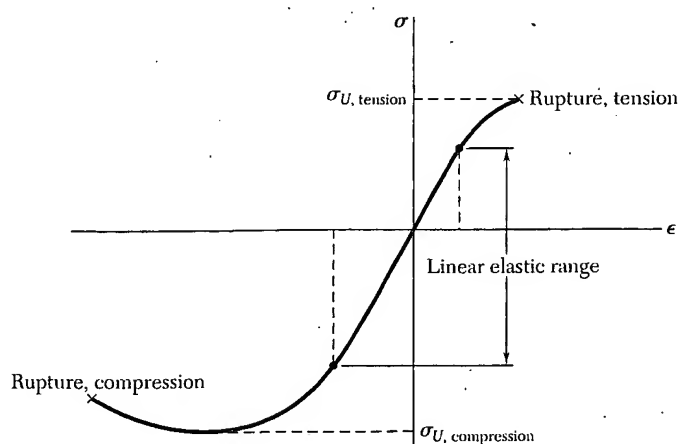


Fig. 2.14 Stress-strain diagram for concrete.

An example of brittle material with different properties in tension and compression is provided by *concrete*, whose stress-strain diagram is shown in Fig. 2.14. On the tension side of the diagram, we first observe a linear elastic range in which the strain is proportional to the stress. After the yield point has been reached, the strain increases faster than the stress until rupture occurs. The behavior of the material in compression is different. First, the linear elastic range is significantly larger. Second, rupture does not occur as the stress reaches its maximum value. Instead, the stress decreases in magnitude while the strain keeps increasing until rupture occurs. Note that the modulus of elasticity, which is represented by the slope of the stress-strain curve in its linear portion, is the same in tension and compression. This is true of most brittle materials.

## \*2.4. TRUE STRESS AND TRUE STRAIN

We recall that the stress plotted in the diagrams of Figs. 2.9 and 2.11 was obtained by dividing the load  $P$  by the cross-sectional area  $A_0$  of the specimen measured before any deformation had taken place. Since the cross-sectional area of the specimen decreases as  $P$  increases, the stress plotted in our diagrams does not represent the actual stress in the specimen. The difference between the *engineering stress*  $\sigma = P/A_0$  that we have computed and the *true stress*  $\sigma_t = P/A$  obtained by dividing  $P$  by the cross-sectional area  $A$  of the deformed specimen becomes apparent in ductile materials after yield has started. While the engineering stress  $\sigma$ , which is directly proportional to the load  $P$ , decreases with  $P$  during the necking phase, the true stress  $\sigma_t$ , which is proportional to  $P$  but also inversely proportional to  $A$ , is observed to keep increasing until rupture of the specimen occurs.

Many scientists also use a definition of strain different from that of the *engineering strain*  $\epsilon = \delta/L_0$ . Instead of using the total elongation  $\delta$  and the original value  $L_0$  of the gage length, they use all the successive values of  $L$  that they have recorded. Dividing each increment  $\Delta L$  of the distance between the gage marks, by the corresponding value of  $L$ , they obtain the elementary strain  $\Delta\epsilon = \Delta L/L$ . Adding the successive values of  $\Delta\epsilon$ , they define the *true strain*  $\epsilon_t$ :

$$\epsilon_t = \sum \Delta\epsilon = \sum (\Delta L/L)$$

With the summation replaced by an integral, they can also express the true strain as follows:

$$\epsilon_t = \int_{L_0}^L \frac{dL}{L} = \ln \frac{L}{L_0} \quad (2.3)$$

The diagram obtained by plotting true stress versus true strain (Fig. 2.15) reflects more accurately the behavior of the material. As we have already noted, there is no decrease in true stress during the necking phase. Also, the results obtained from tensile and from compressive

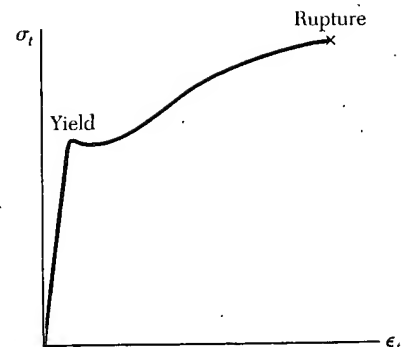


Fig. 2.15 True stress versus true strain for a typical ductile material.

tests will yield essentially the same plot when true stress and true strain are used. This is not the case for large values of the strain when the engineering stress is plotted versus the engineering strain. However, engineers, whose responsibility is to determine whether a load  $P$  will produce an acceptable stress and an acceptable deformation in a given member, will want to use a diagram based on the engineering stress  $\sigma = P/A_0$  and the engineering strain  $\epsilon = \delta/L_0$ , since these expressions involve data that are available to them, namely the cross-sectional area  $A_0$  and the length  $L_0$  of the member in its undeformed state.

## 2.5. HOOKE'S LAW; MODULUS OF ELASTICITY

Most engineering structures are designed to undergo relatively small deformations, involving only the straight-line portion of the corresponding stress-strain diagram. For that initial portion of the diagram (Fig. 2.9), the stress  $\sigma$  is directly proportional to the strain  $\epsilon$ , and we can write

$$\sigma = E\epsilon \quad (2.4)$$

This relation is known as *Hooke's law*, after the English mathematician Robert Hooke (1635–1703). The coefficient  $E$  is called the *modulus of elasticity* of the material involved, or also *Young's modulus*, after the English scientist Thomas Young (1773–1829). Since the strain  $\epsilon$  is a dimensionless quantity, the modulus  $E$  is expressed in the same units as the stress  $\sigma$ , namely in pascals or one of its multiples if SI units are used, and in psi or ksi if U.S. customary units are used.

The largest value of the stress for which Hooke's law can be used for a given material is known as the *proportional limit* of that material. In the case of ductile materials possessing a well-defined yield point, as in Fig. 2.9a, the proportional limit almost coincides with the yield point. For other materials, the proportional limit cannot be defined as easily, since it is difficult to determine with accuracy the value of the stress  $\sigma$  for which the relation between  $\sigma$  and  $\epsilon$  ceases to be linear. But from this very difficulty we can conclude for such materials that using Hooke's law for values of the stress slightly larger than the actual proportional limit will not result in any significant error.

Some of the physical properties of structural metals, such as strength, ductility, and corrosion resistance, can be greatly affected by alloying, heat treatment, and the manufacturing process used. For example, we note from the stress-strain diagrams of pure iron and of three different grades of steel (Fig. 2.16) that large variations in the yield strength, ultimate strength, and final strain (ductility) exist among these four metals. All of them, however, possess the same modulus of elasticity; in other words, their “stiffness,” or ability to resist a deformation within the linear range, is the same. Therefore, if a high-strength steel is substituted for a lower-strength steel in a given structure, and if all dimensions are kept the same, the structure will have an increased load-carrying capacity, but its stiffness will remain unchanged.

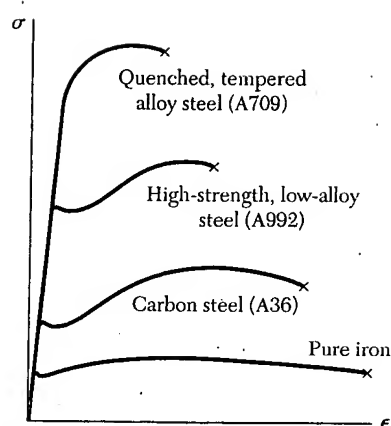


Fig. 2.16 Stress-strain diagrams for iron and different grades of steel.

For each of the materials considered so far, the relation between normal stress and normal strain,  $\sigma = E\epsilon$ , is independent of the direction of loading. This is because the mechanical properties of each material, including its modulus of elasticity  $E$ , are independent of the direction considered. Such materials are said to be *isotropic*. Materials whose properties depend upon the direction considered are said to be *anisotropic*. An important class of anisotropic materials consists of *fiber-reinforced composite materials*.

These composite materials are obtained by embedding fibers of a strong, stiff material into a weaker, softer material, referred to as a *matrix*. Typical materials used as fibers are graphite, glass, and polymers, while various types of resins are used as a matrix. Figure 2.17 shows a layer, or *lamina*, of a composite material consisting of a large number of parallel fibers embedded in a matrix. An axial load applied to the lamina along the  $x$  axis, that is, in a direction parallel to the fibers, will create a normal stress  $\sigma_x$  in the lamina and a corresponding normal strain  $\epsilon_x$  which will satisfy Hooke's law as the load is increased and as long as the elastic limit of the lamina is not exceeded. Similarly, an axial load applied along the  $y$  axis, that is, in a direction perpendicular to the lamina, will create a normal stress  $\sigma_y$  and a normal strain  $\epsilon_y$  satisfying Hooke's law, and an axial load applied along the  $z$  axis will create a normal stress  $\sigma_z$  and a normal strain  $\epsilon_z$  which again satisfy Hooke's law. However, the moduli of elasticity  $E_x$ ,  $E_y$ , and  $E_z$  corresponding, respectively, to each of the above loadings will be different. Because the fibers are parallel to the  $x$  axis, the lamina will offer a much stronger resistance to a loading directed along the  $x$  axis than to a loading directed along the  $y$  or  $z$  axis, and  $E_x$  will be much larger than either  $E_y$  or  $E_z$ .

A flat *laminate* is obtained by superposing a number of layers or laminae. If the laminate is to be subjected only to an axial load causing tension, the fibers in all layers should have the same orientation as the load in order to obtain the greatest possible strength. But if the laminate may be in compression, the matrix material may not be sufficiently strong to prevent the fibers from kinking or buckling. The lateral stability of the laminate may then be increased by positioning some of the layers so that their fibers will be perpendicular to the load. Positioning some layers so that their fibers are oriented at  $30^\circ$ ,  $45^\circ$ , or  $60^\circ$  to the load may also be used to increase the resistance of the laminate to in-plane shear. Fiber-reinforced composite materials will be further discussed in Sec. 2.16, where their behavior under multiaxial loadings will be considered.

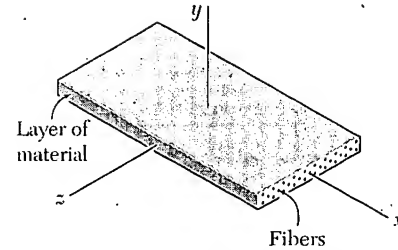


Fig. 2.17 Layer of fiber-reinforced composite material.

## 2.6. ELASTIC VERSUS PLASTIC BEHAVIOR OF A MATERIAL

If the strains caused in a test specimen by the application of a given load disappear when the load is removed, the material is said to behave *elastically*. The largest value of the stress for which the material behaves elastically is called the *elastic limit* of the material.

If the material has a well-defined yield point as in Fig. 2.9a, the elastic limit, the proportional limit (Sec. 2.5), and the yield point are essentially equal. In other words, the material behaves elastically and

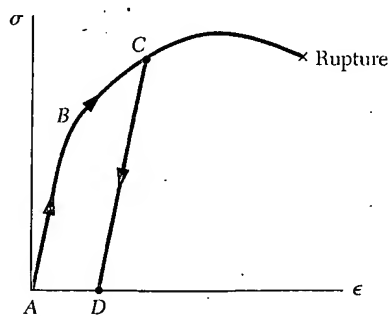


Fig. 2.18

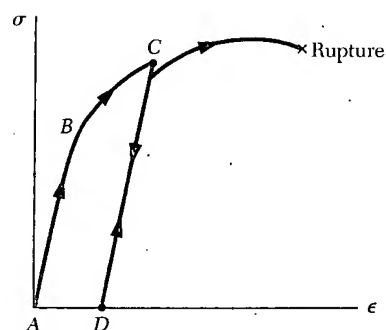


Fig. 2.19

linearly as long as the stress is kept below the yield point. If the yield point is reached, however, yield takes place as described in Sec. 2.3 and, when the load is removed, the stress and strain decrease in a linear fashion, along a line  $CD$  parallel to the straight-line portion  $AB$  of the loading curve (Fig. 2.18). The fact that  $\epsilon$  does not return to zero after the load has been removed indicates that a *permanent set* or *plastic deformation* of the material has taken place. For most materials, the plastic deformation depends not only upon the maximum value reached by the stress, but also upon the time elapsed before the load is removed. The stress-dependent part of the plastic deformation is referred to as *slip*, and the time-dependent part—which is also influenced by the temperature—as *creep*.

When a material does not possess a well-defined yield point, the elastic limit cannot be determined with precision. However, assuming the elastic limit equal to the yield strength as defined by the offset method (Sec. 2.3) results in only a small error. Indeed, referring to Fig. 2.13, we note that the straight line used to determine point  $Y$  also represents the unloading curve after a maximum stress  $\sigma_y$  has been reached. While the material does not behave truly elastically, the resulting plastic strain is as small as the selected offset.

If, after being loaded and unloaded (Fig. 2.19), the test specimen is loaded again, the new loading curve will closely follow the earlier unloading curve until it almost reaches point  $C$ ; it will then bend to the right and connect with the curved portion of the original stress-strain diagram. We note that the straight-line portion of the new loading curve is longer than the corresponding portion of the initial one. Thus, the proportional limit and the elastic limit have increased as a result of the strain-hardening that occurred during the earlier loading of the specimen. However, since the point of rupture  $R$  remains unchanged, the ductility of the specimen, which should now be measured from point  $D$ , has decreased.

We have assumed in our discussion that the specimen was loaded twice in the same direction, i.e., that both loads were tensile loads. Let us now consider the case when the second load is applied in a direction opposite to that of the first one.

We assume that the material is mild steel, for which the yield strength is the same in tension and in compression. The initial load is tensile and is applied until point  $C$  has been reached on the stress-strain diagram (Fig. 2.20). After unloading (point  $D$ ), a compressive load is applied, causing the material to reach point  $H$ , where the stress is equal to  $-\sigma_y$ . We note that portion  $DH$  of the stress-strain diagram is curved and does not show any clearly defined yield point. This is referred to as the *Bauschinger effect*. As the compressive load is maintained, the material yields along line  $HJ$ .

If the load is removed after point  $J$  has been reached, the stress returns to zero along line  $JK$ , and we note that the slope of  $JK$  is equal to the modulus of elasticity  $E$ . The resulting permanent set  $AK$  may be positive, negative, or zero, depending upon the lengths of the segments  $BC$  and  $HJ$ . If a tensile load is applied again to the test specimen, the portion of the stress-strain diagram beginning at  $K$  (dashed line) will curve up and to the right until the yield stress  $\sigma_y$  has been reached.

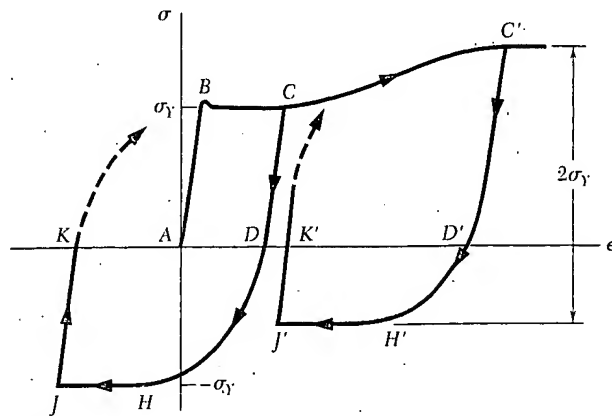


Fig. 2.20

If the initial loading is large enough to cause strain-hardening of the material (point  $C'$ ), unloading takes place along line  $C'D'$ . As the reverse load is applied, the stress becomes compressive, reaching its maximum value at  $H'$  and maintaining it as the material yields along line  $H'J'$ . We note that while the maximum value of the compressive stress is less than  $\sigma_y$ , the total change in stress between  $C'$  and  $H'$  is still equal to  $2\sigma_y$ .

If point  $K$  or  $K'$  coincides with the origin  $A$  of the diagram, the permanent set is equal to zero, and the specimen may appear to have returned to its original condition. However, internal changes will have taken place and, while the same loading sequence may be repeated, the specimen will rupture without any warning after relatively few repetitions. This indicates that the excessive plastic deformations to which the specimen was subjected have caused a radical change in the characteristics of the material. Reverse loadings into the plastic range, therefore, are seldom allowed, and only under carefully controlled conditions. Such situations occur in the straightening of damaged material and in the final alignment of a structure or machine.

## 2.7. REPEATED LOADINGS; FATIGUE

In the preceding sections we have considered the behavior of a test specimen subjected to an axial loading. We recall that, if the maximum stress in the specimen does not exceed the elastic limit of the material, the specimen returns to its initial condition when the load is removed. You might conclude that a given loading may be repeated many times, provided that the stresses remain in the elastic range. Such a conclusion is correct for loadings repeated a few dozen or even a few hundred times. However, as you will see, it is not correct when loadings are repeated thousands or millions of times. In such cases rupture will occur at a stress much lower than the static breaking strength; this phenomenon is known as *fatigue*. A fatigue failure is of a brittle nature, even for materials that are normally ductile.

# REVIEW AND SUMMARY FOR CHAPTER 2

This chapter was devoted to the introduction of the concept of *strain*, to the discussion of the relationship between stress and strain in various types of materials, and to the determination of the deformations of structural components under axial loading.

Considering a rod of length  $L$  and uniform cross section and denoting by  $\delta$  its deformation under an axial load  $P$  (Fig. 2.1), we defined the *normal strain*  $\epsilon$  in the rod as the *deformation per unit length* [Sec. 2.2]:

$$\epsilon = \frac{\delta}{L} \quad (2.1)$$

In the case of a rod of variable cross section, the normal strain was defined at any given point  $Q$  by considering a small element of rod at  $Q$ . Denoting by  $\Delta x$  the length of the element and by  $\Delta \delta$  its deformation under the given load, we wrote

$$\epsilon = \lim_{\Delta x \rightarrow 0} \frac{\Delta \delta}{\Delta x} = \frac{d\delta}{dx} \quad (2.2)$$

Plotting the stress  $\sigma$  versus the strain  $\epsilon$  as the load increased, we obtained a *stress-strain diagram* for the material used [Sec. 2.3]. From such a diagram, we were able to distinguish between *brittle* and *ductile* materials: A specimen made of a brittle material ruptures without any noticeable prior change in the rate of elongation (Fig. 2.11), while a specimen made of a ductile material *yields* after a critical stress  $\sigma_Y$ , called the *yield strength*, has been reached, i.e., the specimen undergoes a large deformation before rupturing, with a relatively small increase in the applied load (Fig. 2.9). An example of brittle material with different properties in tension and in compression was provided by *concrete*.

Normal strain

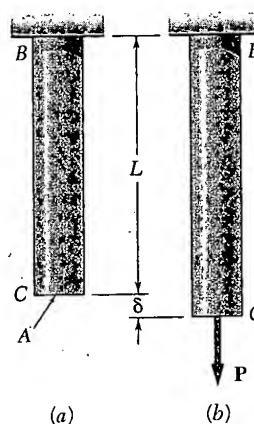


Fig. 2.1

Stress-strain diagram

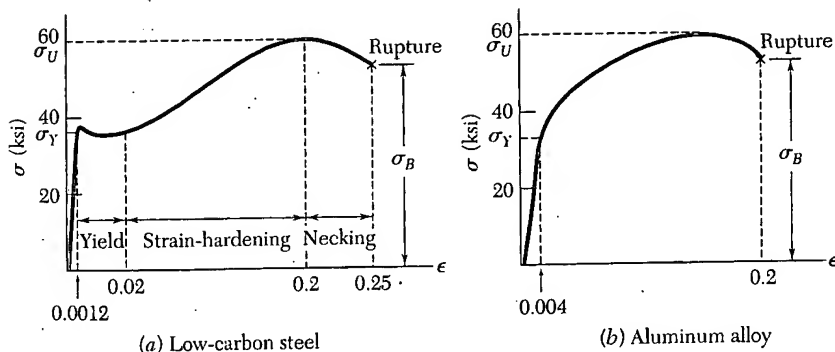


Fig. 2.9

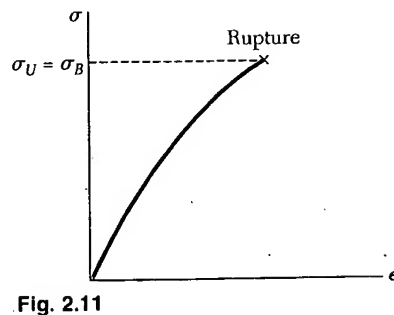


Fig. 2.11



Hooke's law  
Modulus of elasticity

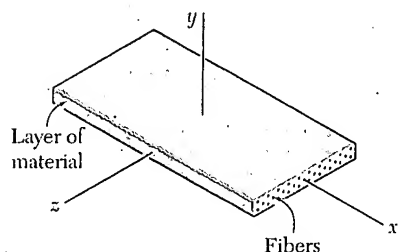


Fig. 2.17

Elastic limit. Plastic deformation

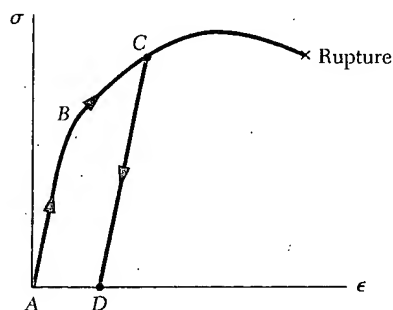


Fig. 2.18

Fatigue. Endurance limit

Elastic deformation under axial loading

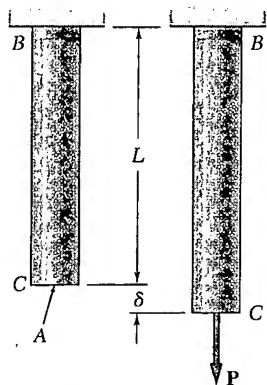


Fig. 2.22

We noted in Sec. 2.5 that the initial portion of the stress-strain diagram is a straight line. This means that for small deformations, the stress is directly proportional to the strain:

$$\sigma = E\epsilon \quad (2.4)$$

This relation is known as *Hooke's law* and the coefficient  $E$  as the *modulus of elasticity* of the material. The largest stress for which Eq. (2.4) applies is the *proportional limit* of the material.

Materials considered up to this point were *isotropic*, i.e., their properties were independent of direction. In Sec. 2.5 we also considered a class of *anisotropic* materials, i.e., materials whose properties depend upon direction. They were *fiber-reinforced composite materials*, made of fibers of a strong, stiff material embedded in layers of a weaker, softer material (Fig. 2.17). We saw that different moduli of elasticity had to be used, depending upon the direction of loading.

If the strains caused in a test specimen by the application of a given load disappear when the load is removed, the material is said to behave *elastically*, and the largest stress for which this occurs is called the *elastic limit* of the material [Sec. 2.6]. If the elastic limit is exceeded, the stress and strain decrease in a linear fashion when the load is removed and the strain does not return to zero (Fig. 2.18), indicating that a *permanent set* or *plastic deformation* of the material has taken place.

In Sec. 2.7, we discussed the phenomenon of *fatigue*, which causes the failure of structural or machine components after a very large number of repeated loadings, even though the stresses remain in the elastic range. A standard fatigue test consists in determining the number  $n$  of successive loading-and-unloading cycles required to cause the failure of a specimen for any given maximum stress level  $\sigma$ , and plotting the resulting  $\sigma$ - $n$  curve. The value of  $\sigma$  for which failure does not occur, even for an indefinitely large number of cycles, is known as the *endurance limit* of the material used in the test.

Section 2.8 was devoted to the determination of the elastic deformations of various types of machine and structural components under various conditions of axial loading. We saw that if a rod of length  $L$  and uniform cross section of area  $A$  is subjected at its end to a centric axial load  $P$  (Fig. 2.22), the corresponding deformation is

$$\delta = \frac{PL}{AE} \quad (2.7)$$

If the rod is loaded at several points or consists of several parts of various cross sections and possibly of different materials, the deformation  $\delta$  of the rod must be expressed as the sum of the deformations of its component parts [Example 2.01]:

$$\delta = \sum_i \frac{P_i L_i}{A_i E_i} \quad (2.8)$$



Fiber-reinforced composite materials

Saint-Venant's principle

Stress concentrations

Plastic deformations

$E$ ,  $\nu$ , and  $G$  are not independent; they satisfy the relation:

$$\frac{E}{2G} = 1 + \nu \quad (2.43)$$

which may be used to determine any of the three constants in terms of the other two.

Stress-strain relationships for fiber-reinforced composite materials were discussed in an optional section (Sec. 2.16). Equations similar to Eqs. (2.28) and (2.36, 37) were derived for these materials, but we noted that direction-dependent moduli of elasticity, Poisson's ratios, and moduli of rigidity had to be used.

In Sec. 2.17, we discussed *Saint-Venant's principle*, which states that except in the immediate vicinity of the points of application of the loads, the distribution of stresses in a given member is independent of the actual mode of application of the loads. This principle makes it possible to assume a uniform distribution of stresses in a member subjected to concentrated axial loads, except close to the points of application of the loads, where stress concentrations will occur.

Stress concentrations will also occur in structural members near a discontinuity, such as a hole or a sudden change in cross section [Sec. 2.18]. The ratio of the maximum value of the stress occurring near the discontinuity over the average stress computed in the critical section is referred to as the *stress-concentration factor* of the discontinuity and is denoted by  $K$ :

$$K = \frac{\sigma_{\max}}{\sigma_{\text{ave}}} \quad (2.48)$$

Values of  $K$  for circular holes and fillets in flat bars were given in Fig. 2.64 on p. 108.

In Sec. 2.19, we discussed the *plastic deformations* which occur in structural members made of a ductile material when the stresses in some part of the member exceed the yield strength of the material. Our analysis was carried out for an idealized *elastoplastic material* characterized by the stress-strain diagram shown in Fig. 2.65

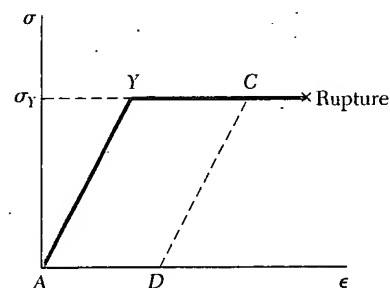


Fig. 2.65

[Examples 2.13, 2.14, and 2.15]. Finally, in Sec. 2.20, we observed that when an indeterminate structure undergoes plastic deformations, the stresses do not, in general, return to zero after the load has been removed. The stresses remaining in the various parts of the structure are called *residual stresses* and may be determined by adding the maximum stresses reached during the loading phase and the reverse stresses corresponding to the unloading phase [Example 2.16].

**This Page is Inserted by IFW Indexing and Scanning  
Operations and is not part of the Official Record**

**BEST AVAILABLE IMAGES**

Defective images within this document are accurate representations of the original documents submitted by the applicant.

Defects in the images include but are not limited to the items checked:

☒ **BLACK BORDERS**

☐ **IMAGE CUT OFF AT TOP, BOTTOM OR SIDES**

☒ **FADED TEXT OR DRAWING**

☐ **BLURRED OR ILLEGIBLE TEXT OR DRAWING**

☐ **SKEWED/SLANTED IMAGES**

☐ **COLOR OR BLACK AND WHITE PHOTOGRAPHS**

☒ **GRAY SCALE DOCUMENTS**

☐ **LINES OR MARKS ON ORIGINAL DOCUMENT**

☐ **REFERENCE(S) OR EXHIBIT(S) SUBMITTED ARE POOR QUALITY**

☐ **OTHER:** \_\_\_\_\_

**IMAGES ARE BEST AVAILABLE COPY.**

**As rescanning these documents will not correct the image problems checked, please do not report these problems to the IFW Image Problem Mailbox.**